Letters

An Interoperable Dynamic Wireless Charging System With Stable Output Based on a Self-Adaptive Two-Pole Receiver

Yiming Zhang, *Senior Member, IEEE*, Hangyan Zhou, Zhiwei Shen, Ronghuan Xie, *Graduate Student Member, IEEE*, Xiaoying Chen, *Member, IEEE*, and Xingkui Mao, *Member, IEEE*

***Abstract*—Dynamic wireless power transfer (DWPT) for electrical vehicles (EVs) is a promising technology that can alleviate mileage anxiety and address onboard battery capacity limitations. However, there are power fluctuation and interoperability problems in DWPT systems. In order to solve these two issues, this letter proposes a decoupling self-adaptive two-pole interoperable receiver. The receiver coils are decoupled by partial overlapping. During the EV movement, the receiver coil can automatically change its polarity according to the mutual inductance variation. In this way, the secondary-side rectifier presents a series or parallel connection and produces a smooth equivalent mutual inductance fluctuation within the moving range, thus achieving a smooth output. Meanwhile, the proposed receiver can be tolerant with the unipolar and bipolar transmitter coils, capable of outputting the same power level and high transmission efficiency. The experimental results validate the effectiveness of the proposed DWPT system.**

***Index Terms*—Dynamic wireless power transfer (DWPT), interoperable, self-adaptive two-pole receiver(Rx), stable output voltage.**

I. Introduction

WIRELESS power transfer (WPT) has received increasing attention from both academia and industry, overcoming some of the drawbacks of conventional wired charging, such as lack of flexibility and electrical shock hazards. Its potential as a promising technology has been identified in different applications, including electric vehicles (EVs), consumer electronics, and biomedical and underwater applications [1], [2], [3], [4], [5], [6], [7]. In recent years, dynamic wireless power transfer (DWPT) [8], [9] has emerged in the context of the rapid development of EVs, which overcomes the problems of the onboard battery capacity limitation, distance anxiety, and inconvenient charging.

Manuscript received 7 April 2024; revised 15 May 2024; accepted 31 May 2024. Date of publication 4 June 2024; date of current version 4 September 2024. This work was supported in part by the National Natural Science Foundation of China under Grant 52107183 and in part by the Natural Science Foundation of Fujian Province under Grant 2022J06011. *(Corresponding authors: Xiaoying Chen; Xingkui Mao.)*

The authors are with the School of Electrical Engineering and Automation, Fuzhou University, Fuzhou 350108, China (e-mail: zym@fzu.edu.cn; 220127134@fzu.edu.cn; 210127138@fzu.edu.cn; 230127018@fzu.edu.cn; fzucxy@fzu.edu.cn; mxk782@fzu.edu.cn).

Color versions of one or more figures in this article are available at https://doi.org/10.1109/TPEL.2024.3409368.

Digital Object Identifier 10.1109/TPEL.2024.3409368

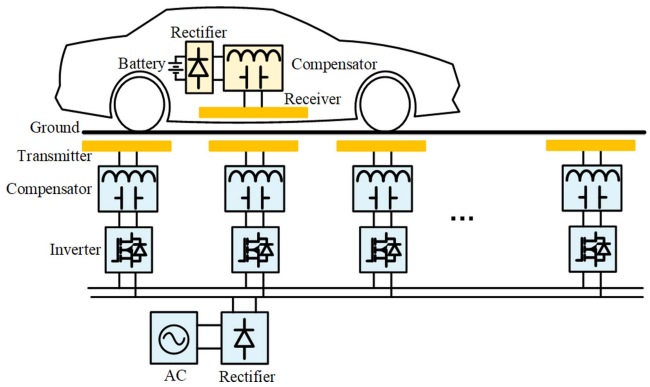

Fig. 1. DWPT system with segmented Txs.

In terms of transmitters (Txs), DWPT can be categorized into two types: long-track Tx [10], [11], [12] and segmented Tx [13], [14], [15], [16]. The former can power multiple receivers (Rxs) simultaneously and has a simpler circuit and coil structure. However, its coupling performance is poor and inefficient, and the high leakage magnetic field can lead to electromagnetic interference (EMI). Txs of the latter shown in Fig. 1 are controllable and switchable, which can be turned ON or OFF according to the position of the Rx, and it is capable of achieving higher efficiency and lower EMI. But in practice, it still has some critical problems that need to be solved. One is that it requires more inverters and compensation components, which will generate higher construction costs. The second is the performance stability of in-motion EVs in terms of efficiency and output power during EV traveling.

In a segmented Tx DWPT system, a large distance is usually set between adjacent Txs to eliminate cross coupling and to decouple the Txs, making it easy to control and implement. However, this inevitably leads to fluctuations in motion efficiency and output power, which shortens the battery life and reduces its operational stability. Nowadays, many studies are carried out on the output power fluctuation problem of DWPT systems. One is that the output power can be regulated in real time by

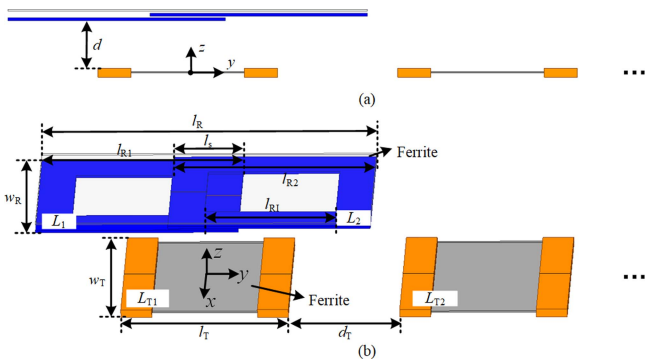

Fig. 2. Proposed magnetic couplers. (a) Front view. (b) 3-D view.

adding control modules [17], [18]. The second is that the mutual inductance change during the moving process can be smoothed by designing a magnetic coupler structure. A grouped periodic series spiral coupler was proposed [19] to make the dynamic charging relatively stable. Unipolar and bipolar coils were laid alternately [20] to form a segmented Tx, effectively smoothing the mutual inductance variations. Multiple rectangular unipolar coils were closely placed as Txs to reduce mutual inductance fluctuations [21]. Bipolar coils placed symmetrically on unipolar Tx coils are able to decouple adjacent Txs and enable stable mutual inductance [22]. All the aforementioned studies have been conducted for the Tx. The tightly spaced Tx not only creates cross coupling but also leads to higher construction costs. In addition, the laying of Tx coils with different polarities will be incompatible with Rx coils produced by different manufacturers, thus inevitably creating interoperability.

Therefore, in order to solve the problems of output power fluctuation and interoperability, a mutually decoupled self-adaptive two-pole interoperable Rx is proposed in this letter. During EV traveling, the Rx can automatically change its connection mode, i.e., series or parallel, according to its respective polarities. This adaptive mode not only smooths the mutual inductance fluctuation during motion but also is compatible with Txs of different polarities, making them interoperable. In addition, the smooth mutual inductance fluctuation broadens the range of Rx motion, allowing the Tx to be loosely arranged and naturally decoupled, which reduces the laying cost and simplifies the system design at the same time.

II. System Modeling and Analysis

A. Magnetic Coupler

The structure of the proposed mutually decoupled two-pole interoperable magnetic coupler is shown in Fig. 2. L_1 and L_2 are the two poles of the Rx, achieving decoupling by partial overlapping. A segmented solenoid pad is used for the Tx due to its better misalignment performance and higher coupling [23], [24]. The physical parameters are given in Table I. When the overlap length l_s is 126 mm, the cross-coupling coefficient $k_{12} < 0.01$. The number of turns of L_1 and L_2 is set to 15, and the number of turns of the windings on the left and right sides of L_{Ti} $(i = 1, 2, \ldots, n)$ is 13.

TABLE I
Parameters of the Magnetic Coupler

Parameter	Description	Value
d	Air gap	80 mm
l_R	Length of the Rx	600 mm
l_{R1}	Length of L_1	363 mm
l_{R2}	Length of L_2	363 mm
l_{RI}	Inner length of L_1/L_2	236.5 mm
l_s	Length of the overlap	126 mm
w_R	Width of the Rx	300 mm
w_T	Width of the Tx	300 mm
l_T	Length of the Tx	300 mm
d_T	Distance between two Txs	200 mm

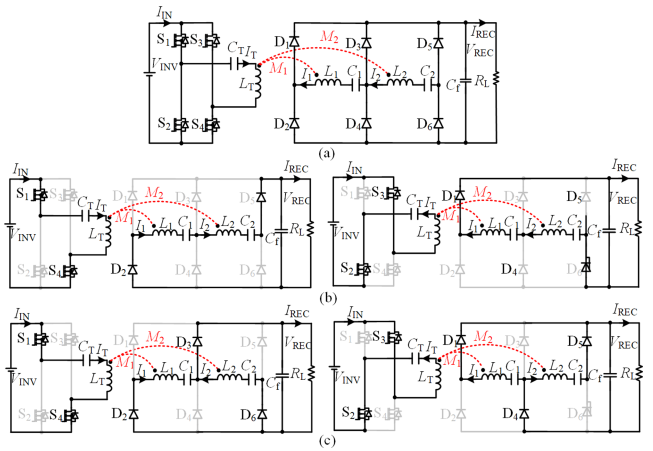

Fig. 3. Circuit topology of the proposed DWPT system with stable output characteristics. (a) Overall circuit topology. (b) Current path when M_1 and M_2 are of the same polarity. (c) Current path when M_1 and M_2 are of different polarity.

To illustrate the interoperability of the proposed system, the Tx can be set up as a bipolar coil with a length of 400 mm, a width of 300 mm, and a number of turns of 8 and a unipolar coil with a length of 200 mm, a width of 300 mm, and a number of turns of 10. The simulated and measured equivalent mutual inductance fluctuations are given in Section III.

B. Circuit Topology

The circuit topology of the proposed DWPT system with stable output characteristics is shown in Fig. 3, where V_{INV} and I_{IN} are the input dc voltage and dc current, respectively; V_{REC} and I_{REC} are the charging voltage and charging current, respectively; R_{L} is the load resistor; L_{T} is the Tx coil; L_1 and L_2 are the Rx coils; and C_{T}, C_1, and C_2 are the series compensating capacitors for the Tx and the Rx. I_{T}, I_1, and I_2 are the currents flowing through the Tx and Rx coils; M_i is the mutual inductance between L_{T} and L_i $(i = 1, 2)$. Due to the decoupling of the Rx coils, the cross coupling of L_1 and L_2 is negligible.

The polarities of M_1 and M_2 will be changed during the movement of the Rx: when M_1 and M_2 are of the same polarity, L_1 and L_2 are connected in series, with the current flow path, as shown in Fig. 3(b); when the polarities of M_1 and M_2 are opposite, L_1 and L_2 are connected in parallel, with the current flow path, as shown in Fig. 3(c). In summary, it can be seen

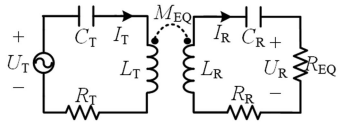

Fig. 4. Simplified equivalent circuit of the proposed DWPT system.

that the proposed adaptive rectifier will automatically change its connection according to the change of mutual inductance, where the equivalent mutual inductance in different operating modes can be summarized as follows:

$$M_{\mathrm{EQ}} = \begin{cases} |M_1 + M_2|, (M_1, M_2 > 0 \text{or} M_1, M_2 < 0) \\ \max\{|M_1|, |M_2|\}, (M_1 < 0, M_2 > 0 \text{or} M_1 > 0, M_2 < 0) \end{cases}. \tag{1}$$

Benefiting from the adaptive nature, this rectifier allows the DWPT system to maintain stable equivalent mutual inductance fluctuations. Moreover, the variability of the polarity of M_1 and M_2 makes the system interoperable and compatible with the Tx of different polarities, as will be verified in Section III.

The simplified equivalent circuit of the system is shown in Fig. 4, which can ultimately be equated to the series–series topology. R_{T} and R_{R} are the equivalent series resistances (ESRs) of the Tx and Rx loops, respectively. U_{T} and U_{R} are the fundamental components of the inverter and rectifier ac voltages, respectively. R_{EQ} is the equivalent ac load resistance. M_{EQ} is the equivalent mutual inductance of the Tx and Rx coils, which depends on the polarity of the Tx coil. The formulas for U_{T}, U_{R}, and R_{EQ} are as follows:

$$U_{\mathrm{T}} = \frac{2\sqrt{2}}{\pi} V_{\mathrm{INV}}, \quad U_{\mathrm{R}} = \frac{2\sqrt{2}}{\pi} V_{\mathrm{REC}}, \quad R_{\mathrm{EQ}} = \frac{8}{\pi^2} R_{\mathrm{L}}. \tag{2}$$

The WPT system operates at the resonance frequency ω_0

$$\omega_0 = \frac{1}{\sqrt{L_{\mathrm{T}} C_{\mathrm{T}}}} = \frac{1}{\sqrt{L_1 C_1}} = \frac{1}{\sqrt{L_2 C_2}}. \tag{3}$$

Neglecting the ESRs, the expression for the ac voltage can be obtained using Kirchhoff's voltage law as

$$I_{\mathrm{T}} = \frac{R_{\mathrm{EQ}} U_{\mathrm{T}}}{(\omega M_{\mathrm{EQ}})^2}, \quad I_{\mathrm{R}} = \frac{U_{\mathrm{T}}}{\omega M_{\mathrm{EQ}}}. \tag{4}$$

Thus, the charging voltage V_{REC}, the charging current I_{REC} at the dc side, and the output power can be expressed as

$$I_{\mathrm{REC}} = \frac{8}{\pi^2} \frac{V_{\mathrm{INV}}}{\omega_0 M_{\mathrm{EQ}}}, \quad V_{\mathrm{REC}} = \frac{8}{\pi^2} \frac{V_{\mathrm{INV}} R_{\mathrm{L}}}{\omega_0 M_{\mathrm{EQ}}}. \tag{5}$$

$$P_{\mathrm{out}} = I_{\mathrm{R}}^2 R_{\mathrm{EQ}} = \left[\frac{8}{\pi^2} \frac{V_{\mathrm{INV}}}{\omega M_{\mathrm{EQ}}} \right]^2 R_{\mathrm{L}}. \tag{6}$$

From (6), the output power is only related to the equivalent mutual inductance when the input dc voltage and load are constant. Therefore, a smooth power output can be achieved by keeping the equivalent mutual inductance constant.

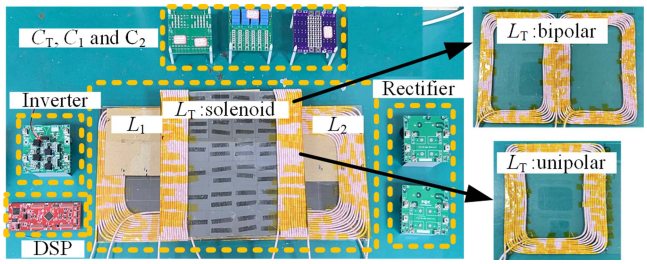

Fig. 5. Photo of the experimental prototype.

TABLE II
PARAMETERS OF THE EXPERIMENTAL PROTOTYPE

Symbol	Value	Symbol	Value
V_{INV}	150 V	R_{L}	20 Ω
L_1	158.49 μH	C_1	22.14 nF
L_2	165.83 μH	C_2	21.16 nF
$L_{\mathrm{T\,(solenoid)}}$	189.12 μH	$C_{\mathrm{T\,(solenoid)}}$	18.56 nF
$L_{\mathrm{T\,(unipolar)}}$	58.24 μH	$C_{\mathrm{T\,(unipolar)}}$	60.26 nF
$L_{\mathrm{T\,(bipolar)}}$	109.98 μH	$C_{\mathrm{T\,(unipolar)}}$	32 nF

The ac–ac efficiency can be derived as

$$\eta = \frac{I_{\mathrm{R}}^2 R_{\mathrm{EQ}}}{I_{\mathrm{R}}^2 R_{\mathrm{EQ}} + I_{\mathrm{T}}^2 R_{\mathrm{T}} + I_{\mathrm{R}}^2 R_{\mathrm{R}}}. \tag{7}$$

III. EXPERIMENTAL VALIDATION

The experimental prototype of the proposed DWPT system is shown in Fig. 5, where the Tx can be set as solenoid, unipolar, and bipolar coils. The parameters of the experimental prototype are shown in Table II. The measured mutual inductance and coupling coefficient between L_1 and L_2 are 1.17 μH and 0.007, respectively, indicating the realization of decoupling between L_1 and L_2.

The mutual inductance fluctuation curves for the three Txs can be obtained by FEA, and corresponding M_{EQ} can be calculated and measured, as shown in Fig. 6(a)–(c). It can be seen that the adaptivity of the proposed Rx is able to transform the original violently fluctuating M_1 and M_2 into smoothly fluctuating M_{EQ}. Since Txs are designed with different sizes and spacing, they have different ranges of movement.

Calculated and experimental results of dc–dc efficiency and output power at three Txs are given in Fig. 6(d)–(f). Selecting several representative points for static charging verification within the moving range of the two Txs, it can be seen that the output power of the system fluctuates more smoothly when the Tx is a solenoid coil and a bipolar coil throughout the charging range, which are ±6.4% and ±3.5%, respectively. When the Tx is a unipolar coil, the output power fluctuation is higher at ±14.8%. In addition, the system is interoperable and capable of delivering the same power level.

The experimental waveforms of ac voltage and ac current for three Txs are given in Fig. 7. It can be seen that the zero-voltage switching has been achieved. The experimental results show that the proposed system realizes good interoperability.

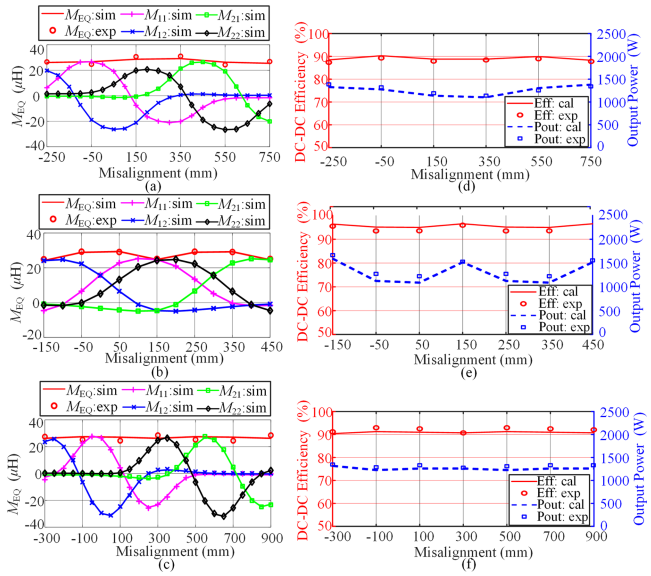

Fig. 6. Simulated and experimental M_{EQ} for (a) solenoid Tx, (b) unipolar Tx, and (c) bipolar Tx. Calculated and experimental results of DC–DC efficiency and output power for (d) solenoid Tx, (e) unipolar Tx, and (f) bipolar Tx.

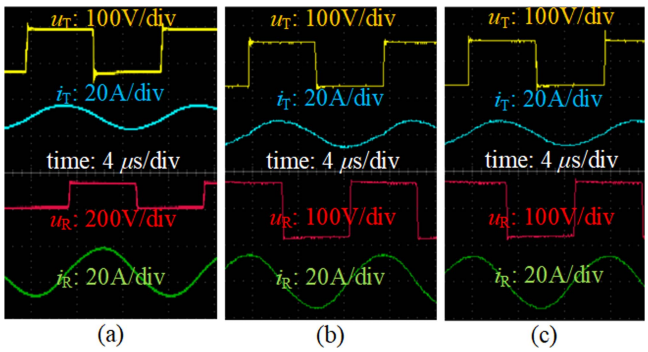

Fig. 7. Experimental waveforms. (a) Tx: Solenoid. (b) Tx: Unipolar. (c) Tx: Bipolar.

TABLE III
COMPARISON WITH THE EXISTING STUDIES

Ref.	Type of Rx	Air gap	Interoperability	Efficiency	Output fluctuations
[13]	Unipolar	50 mm	No	87.6%	±2%
[14]	Unipolar	200 mm	No	91%	±25%
[15]	Unipolar	105 mm	No	85%	±6%
[20]	Unipolar and Bipolar	100 mm	No	90.37%	±2%
[21]	Unipolar	150 mm	No	89.78%	±7.5%
Proposed Rx	Bipolar	80 mm	Yes	95.3%	±3.5%

Table III shows a comparison of the proposed Rx with the existing bipolar or unipolar Rx in terms of efficiency, interoperability, and performance in different air gaps, and it can be seen that the proposed Rx is not only interoperable but also capable of maintaining a smooth output power while having a high efficiency.

IV. CONCLUSION

A mutually decoupled self-adaptive two-pole Rx has been proposed in this letter to solve the output power fluctuation and interoperability problems in DWPT systems. The decoupling of Rx coils is achieved by partial overlapping. The proposed two-pole Rx is able to automatically change its respective polarity in response to the mutual inductance variations occurring during the EV movement, resulting in different connections of the rectifier, i.e., series or parallel. By this adaptive nature, the equivalent mutual inductance is made to maintain a stable value throughout the entire range of movement, thus ensuring smooth output power. In addition, the Rx is interoperable, being able to be compatible with both unipolar and bipolar Tx coils with the same level of output power over a movement range. The experimental results validate the effectiveness of the proposed DWPT system.

REFERENCES

[1] Y. Zhang, Z. Shen, W. Pan, H. Wang, Y. Wu, and X. Mao, "Constant current and constant voltage charging of wireless power transfer system based on three-coil structure," *IEEE Trans. Ind. Electron.*, vol. 70, no. 1, pp. 1066–1070, Jan. 2023.

[2] R. Xie, Y. Wu, H. Tang, Y. Zhuang, and Y. Zhang, "A strongly coupled vehicle-to-vehicle wireless charging system for emergency charging purposes with constant-current and constant-voltage charging capabilities," *IEEE Trans. Power Electron.*, vol. 39, no. 4, pp. 3985–3989, Apr. 2024.

[3] S. Y. Choi, S. Y. Jeong, E. S. Lee, B. W. Gu, S. W. Lee, and C. T. Rim, "Generalized models on self-decoupled dual pick-up coils for a large lateral tolerance," *IEEE Trans. Power Electron.*, vol. 30, no. 11, pp. 6434–6445, Nov. 2015.

[4] W. Pan, C. Liu, H. Tang, Y. Zhuang, and Y. Zhang, "An interoperable electric vehicle wireless charging system based on mutually spliced double-D coil," *IEEE Trans. Power Electron.*, vol. 39, no. 3, pp. 3864–3872, Mar. 2024.

[5] Y. Zhang, S. Chen, X. Li, and Y. Tang, "Design methodology of freepositioning nonoverlapping wireless charging for consumer electronics based on antiparallel windings," *IEEE Trans. Ind. Electron.*, vol. 69, no. 1, pp. 825–834, Jan. 2022.

[6] M. R. Basar, M. Y. Ahmad, J. Cho, and F. Ibrahim, "An improved wearable resonant wireless power transfer system for biomedical capsule endoscope," *IEEE Trans. Ind. Electron.*, vol. 65, no. 10, pp. 7772–7781, Oct. 2018.

[7] Y. Wu, H. Wang, Y. Zhuang, and Y. Zhang, "A shared charging channel for power and auxiliary batteries in electric vehicles," *IEEE Trans. Ind. Electron.*, vol. 71, no. 7, pp. 8202–8206, Jul. 2024.

[8] B. Song, S. Cui, Y. Li, and C. Zhu, "A fast and general method to calculate mutual inductance for EV dynamic wireless charging system," *IEEE Trans. Power Electron.*, vol. 36, no. 3, pp. 2696–2709, Mar. 2021.

[9] W. Liu, K. T. Chau, C. H. T. Lee, C. Jiang, and W. Han, "A switched-capacitorless energy-encrypted transmitter for roadway-charging electric vehicles," *IEEE Trans. Magn.*, vol. 54, no. 11, Nov. 2018, Art. no. 8401006.

[10] A. Zaheer, G. A. Covic, and D. Kacprzak, "A bipolar pad in a 10-kHz 300-W distributed IPT system for AGV applications," *IEEE Trans. Ind. Electron.*, vol. 61, no. 7, pp. 3288–3301, Jul. 2014.

[11] S. Y. Choi, B. W. Gu, S. Y. Jeong, and C. T. Rim, "Advances in wireless power transfer systems for roadway-powered electric vehicles," *IEEE J. Emerg. Sel. Topics Power Electron.*, vol. 3, no. 1, pp. 18–36, Mar. 2015.

[12] V.-B. Vu, M. Dahidah, and V. Pickert, "Efficiency-cost parametric-analysis of a three-phase wireless dynamic charging system for electric vehicles," *IEEE J. Emerg. Sel. Topics Power Electron.*, vol. 3, no. 3, pp. 482–491, Jul. 2022.

[13] C. Cai, M. Saeedifard, J. Wang, P. Zhang, J. Zhao, and Y. Hong, "A cost-effective segmented dynamic wireless charging system with stable efficiency and output power," *IEEE Trans. Power Electron.*, vol. 37, no. 7, pp. 8682–8700, Jul. 2022.

[14] J. Noeren, N. Parspour, and L. Elbracht, "An easily scalable dynamic wireless power transfer system for electric vehicles," *Energies*, vol. 16, no. 9, Jul. 2022, Art. no. 3936.

[15] S. Li, L. Wang, Y. Guo, C. Tao, and L. Ji, "Power stabilization with double transmitting coils and T-type compensation network for dynamic wireless charging of EV," *IEEE J. Emerg. Sel. Topics Power Electron.*, vol. 8, no. 2, pp. 1801–1812, Jun. 2020.

[16] E. S. Lee, M. Y. Kim, S. M. Kang, and S. H. Han, "Segmented IPT coil design for continuous multiple charging of an electrified monorail system," *IEEE Trans. Power Electron.*, vol. 37, no. 3, pp. 3636–3649, Mar. 2022.

[17] F. F. A. van der Pijl, M. Castilla, and P. Bauer, "Adaptive slide-mode control for a multiple-user inductive power transfer system without need for communication," *IEEE Trans. Ind. Electron.*, vol. 60, no. 1, pp. 271–279, Jan. 2013.

[18] A. Ong, P. K. S. Jayathuathnage, J. H. Cheong, and W. L. Goh, "Transmitter pulsation control for dynamic wireless power transfer systems," *IEEE Trans. Transp. Electrific.*, vol. 3, no. 2, pp. 418–426, Jun. 2017.

[19] X. Zhang, Z. Yuan, Q. Yang, Y. Li, J. Zhu, and Y. Li, "Coil design and efficiency analysis for dynamic wireless charging system for electric vehicles," *IEEE Trans. Magn.*, vol. 52, no. 7, Jul. 2016, Art. no. 8700404.

[20] Y. Li et al., "A new coil structure and its optimization design with constant output voltage and constant output current for electric vehicle dynamic wireless charging," *IEEE Trans. Ins. Inform.*, vol. 15, no. 9, pp. 5244–5256, Sep. 2019.

[21] F. Lu, H. Zhang, H. Hofmann, and C. C. Mi, "A dynamic charging system with reduced output power pulsation for electric vehicles," *IEEE Trans. Ind. Electron.*, vol. 63, no. 10, pp. 6580–6590, Oct. 2016.

[22] X. Li, J. Hu, H. Wang, X. Dai, and Y. Sun, "A new coupling structure and position detection method for segmented control dynamic wireless power transfer systems," *IEEE Trans. Power Electron.*, vol. 35, no. 7, pp. 6741–6745, Jul. 2020.

[23] Y. Tang, F. Zhu, Y. Wang, and H. Ma, "Design and optimizations of solenoid magnetic structure for inductive power transfer in EV applications," in *Proc. IEEE 41st Annu. Conf. Ind. Electron. Soc.*, 2015, pp. 1459–1464.

[24] Y. Yao, S. Gao, J. Mai, X. Liu, X. Zhang, and D. Xu, "A novel misalignment tolerant magnetic coupler for electric vehicle wireless charging," *IEEE J. Emerg. Sel. Topics Power Electron.*, vol. 3, no. 2, pp. 219–229, Apr. 2022.